

Stretched reconstruction based on 2D freehand ultrasound for peripheral artery imaging

Thomas Leblanc, Florent Lalys, Quentin Tollenaere, Adrien Kaladji, Antoine Lucas, Antoine Simon

▶ **To cite this version:**

Thomas Leblanc, Florent Lalys, Quentin Tollenaere, Adrien Kaladji, Antoine Lucas, et al.. Stretched reconstruction based on 2D freehand ultrasound for peripheral artery imaging. International Journal of Computer Assisted Radiology and Surgery, 2022, 17 (7), pp.1281-1288. 10.1007/s11548-022-02636-w . hal-03659666

HAL Id: hal-03659666
https://hal.science/hal-03659666

Submitted on 23 Sep 2022

HAL is a multi-disciplinary open access archive for the deposit and dissemination of scientific research documents, whether they are published or not. The documents may come from teaching and research institutions in France or abroad, or from public or private research centers.

L'archive ouverte pluridisciplinaire **HAL**, est destinée au dépôt et à la diffusion de documents scientifiques de niveau recherche, publiés ou non, émanant des établissements d'enseignement et de recherche français ou étrangers, des laboratoires publics ou privés.



Distributed under a Creative Commons Attribution - NonCommercial 4.0 International License

Stretched Reconstruction Based on 2D Freehand Ultrasound for Peripheral Artery Imaging

Thomas Leblanc[1,2], Florent Lalys[1], Quentin Tollenaere[3], Adrien Kaladji[2,4], Antoine Lucas[2,4], Antoine Simon[2]

1. Therenva, F-35000, Rennes, France
2. Univ Rennes, CHU Rennes, CLCC Eugène Marquis, Inserm, LTSI – UMR 1099, F-35000 Rennes, France
3. CHU Rennes, Vascular Medecine Unit, F-35033 Rennes, France
4. CHU Rennes, Department of Cardiothoracic and Vascular Surgery, F-35033 Rennes, France

Abstract

Purpose. Endovascular revascularization is becoming the established first-line treatment of peripheral artery disease (PAD). Ultrasound (US) imaging is used pre-operatively to make the first diagnosis and is often followed by a CT angiography (CTA). US provides a non-invasive and non-ionizing method for the visualization of arteries and lesion(s). This paper proposes to generate a 3D stretched reconstruction of the femoral artery from a sequence of 2D US B-mode frames.

Methods. The proposed method is solely image-based. A Mask-RCNN is used to segment the femoral artery on the 2D US frames. In-plane registration is achieved by aligning the artery segmentation masks. Subsequently, a convolutional neural network (CNN) predicts the out-of-plane translation. After processing all input frames and re-sampling the volume according to the vessel's centerline, the whole femoral artery can be visualized on a single slice of the resulting stretched view.

Results. 111 tracked US sequences of the left or right femoral arteries have been acquired on 18 healthy volunteers. 5-fold cross-validation was used to validate our method and achieve an absolute mean error of 0.28 ± 0.28 mm and a median drift error of 8.98%.

Conclusion. This study demonstrates the feasibility of freehand US stretched reconstruction following a deep learning strategy for imaging the femoral artery. Stretched views are generated and can give rich diagnosis information in the pre-operative planning of PAD procedures. This visualization could replace traditional 3D imaging in the pre-operative planning process, and during the pre-operative diagnosis phase, to identify, locate, and size stenosis/thrombosis lesions.

Keywords: Freehand Ultrasound, Stretched Reconstruction, Endovascular Peripheral Artery Disease

Corresponding author: Thomas Leblanc, email: thomas.leblanc@therenva.com. Tel: +33658017381

Accepted manuscript / Final version

1 Introduction

Lower limb peripheral artery disease (PAD) is a common and serious disease. The treatment of PAD has evolved considerably, with endovascular revascularization techniques becoming the established first-line treatment for peripheral artery lesion(s) [1, 2]. A typical scenario begins with Doppler ultrasound (US) to establish the diagnosis and provide a morphological and hemodynamic description of the lesion(s), Doppler US is indeed the first line imaging technique when discussing revascularization [3]. It is sometimes followed by another morphological examination such as CT angiography (CTA) or, less frequently, MR angiography (MRA). MRA is less accessible and more expensive than other imaging techniques. The main limit of using CTA is the radiation exposure for the patient and the contrast agent injection, which can be contraindicated for some patients due to its nephrotoxicity. However, the CTA is useful to give a 3D visualization of the patient's anatomy to the surgeon. Indeed, the Doppler exam only leads to a Doppler report containing all the hemodynamics measures but does not present a full visualization of the arteries anatomy with localization information. In any case, an arteriography with intent to treat is performed in the operating room (OR). The purpose of this intra-operative angiography is to fully identify and map lesions to be able to navigate and treat them under X-ray fluoroscopic guidance. This phase can be referred to the diagnosis phase. However, angiography and fluoroscopy acquisitions generate high levels of radiation to the patient and medical staff and the use of contrast agent has to be limited due to its nephrotoxicity.

3D US provides a non-invasive and non-ionizing method for the visualization of arteries and could be easily integrated within the patient care. Pre-operatively, 3D US could help to visualize lesions and enhance the diagnosis step. The main disadvantages are their price and limited field of view, preventing the visualization of the whole artery with a single acquisition. Therefore, a variety of US volume reconstruction techniques from a set of 2D US frames have been proposed to compensate for this limitation [4]. Among these methods, mechanical scanning techniques [5] are opposed to freehand scanning approach based on tracking devices [6, 7]. The tracking devices can be optical or electromagnetic and requires a sensor to be attached to the probe. The electromagnetic tracker has a smaller tracking area and suffers from interferences caused by surrounding metal instruments. Concerning the optical tracker, the line of sight of the camera must not be obstructed, which can be annoying for complex scanning trajectories. Freehand US is the most cost-effective and convenient method for reconstruction and offers freedom of movement to the practitioners.

Recently, deep learning-based reconstruction methods have emerged and get rid of tracking systems which can be expensive, cumbersome, and avoid the practitioner's concerns about tracking signals. Prevost *et al.* [8] used a convolutional neural network (CNN) to estimate the relative motion between two consecutives frames in a 2D US sequence to reconstruct an US volume. They used US sequences acquired on phantoms, forearms, and lower legs. The network takes two frames as input and outputs the motion between them in terms of translation (3 axes) and rotation (3 axes). An optical flow field is also computed and stacked with the input pair to improve in-plane motion estimation. In another study, they gave extra information to their network by fixing an inertial measurement unit (IMU) on the probe which helps the network estimating orientations [9]. In the context of transrectal US (TRUS), Dupuy *et al*. registered each 2D US frame with a preoperative US volume by estimating the rotations between the current live 2D US frame and the preceding one [10]. They used a deeper network that also takes a pair of frames as input with the associated optical flow and outputs the relative rotation between them. They give additional information to the network such as the probe tracking sensor information and the prior trajectory information from the last registration result. In [11], a ResNet34 architecture was used as the localization network. They used FlowNet to extract motion features since they observed that the Farnebäck optical flow estimation was not always accurate. Moreover, they add a consistency loss function term used in stereo vision. They showed that their method

Accepted manuscript / Final version

leads to better results than the method of Prevost *et al.* (without IMU), except for the out-of-plane translation. Using TRUS data, with the same purpose of providing more information to the network, a 3D CNN has been designed to take more than two consecutives frames as input to add more temporal information [12]. They used a 3D CNN that takes a volume as input data containing a set of consecutives frames to estimate the global motion between the first and the last frame. Unlike previous works, they did not explicitly give motion features to the network. With a different approach, Luo *et al.* combined a recurrent convolutional LSTM backbone with self-supervised learning and adversarial learning to avoid irregular reconstructions [13]. They proposed an end-to-end online learning framework that enables the global optimization from slice-to-slice transformation to the final volume reconstruction. That leads to more robust results on complex sequences.

In this study, a method to generate a stretched reconstruction of the femoral artery from a sequence of 2D US is proposed without any additional device (tracking device or IMU). In the area of vascular visualization and in the context of PAD, stretched views offer a rich 2D representation of tubular structures from 3D data [14]. By re-sampling the volume according to the vessel's centerline, the target vessel becomes fully visible on a single slice. These views are used to size the lesions as they include relevant information for diagnostic purposes such as artery diameter or length and localization of lesions. The term reconstruction is employed because the US volume is directly built for this view. Even though this technique disregards orientation and leads to anatomical deformations, stretched views offer a sufficient visualization for diagnostic and planning purposes. The femoral artery has indeed very low curvature, the scan trajectory to acquire a sequence on the femoral artery is indeed almost linear. The translation estimate in the longitudinal axis is sufficient to generate stretched views.

2 Method

The proposed method is decomposed into four main steps. The overall workflow is depicted in Fig. 1. Firstly, a Mask R-CNN is used to segment the artery on 2D US frames. The generated segmentation mask allows aligning frames of a pair according to both femoral artery's barycenters. Then, the aligned stacked frames are used as input for a CNN which estimates the out-of-plane translation in the longitudinal axis. Finally, stretched views are generated using the entire 2D sequence. Since the need for artery alignment before longitudinal motion estimation is an open question, the use of the CNN directly on the original frames was also evaluated.

2.1 Ground Truth Acquisition

2D US B-mode sequences were collected on healthy subjects using the Aixplorer® echograph from Supersonic Imagine and an optical tracking device (NDI Polaris Spectra). An optical sensor was fixed on the probe and spatial calibration has been achieved using an N-wire phantom and the PLUS toolkit software [15]. Spatial calibration is indeed required to determine the transformation between a pixel of the US frame and the tracked sensor.

For each frame of the US sequences, a 4x4 transformation matrix was provided by the optical tracking system. In this manner, for each pair of consecutive US frames, two transformation matrices were provided T_i and T_{i+1} corresponding to the position of the first and the second frame, respectively. To assess the relative motion and for axes standardization between the pairs, both transformation matrices were projected on T_i such that the resulting T'_i is the identity and T'_{i+1} the relative displacement between them. t_z was then extracted from T'_{i+1}. It represents the out-of-plane displacement between the frames and served as ground truth.

Accepted manuscript / Final version

111 tracked US sequences (40788 2D frames) of the left or right femoral artery were acquired on 18 healthy volunteers by two different operators. All sequences were recorded from the beginning of the thigh to the knee following the femoral artery (proximal to distal).

2.2 Artery Segmentation and Frame In-Plane Alignment

A Mask R-CNN with inception backbone was used to segment the femoral artery. Trained weights on the COCO dataset were used for initialization. Since there is only one femoral artery in the considered frames, the network was constrained to keep only the mask with the highest detection probability. US sequences were manually annotated using LabelMe [16] to feed the Mask R-CNN. A total of 12 out of the 111 sequences from 6 volunteers were manually segmented. The database was split into 6 (4 volunteers, 2073 frames), 3 (1 volunteer, 702 frames), and 3 (1 volunteer, 1004 frames) sequences for training, validation, and testing, respectively.

The network was optimized with the TensorFlow's Object Detection API using gradient descent with a fixed learning rate of $1x10^{-4}$ and a momentum coefficient of 0.9 to speed up the convergence. Random horizontal flip was used for data augmentation since similar information is present between the frame of the leg and the flipped frame from the other leg. The batch size was set to 1 due to memory limitations. An input size of 688×688 was used to preserve the initial pixel size of 0.056mm to keep the maximum of image information.

Dice scores were calculated between the manual segmentation and the output masks of the network to evaluate the resulting model.

The entire database was segmented using the final trained network. To handle with false negative cases, we performed spatial interpolation of the output masks through the sequences. The position and the shape of masks were linearly interpolated to generate masks on the frames where the network did not detect the artery. The interpolation process stopped when the artery was not detected on more than 10 consecutives frames. In this way, all sequences have been shortened and have been cut when the artery goes too deep and disappears from the US frames. All frames can then be aligned by considering their mask's barycenter.

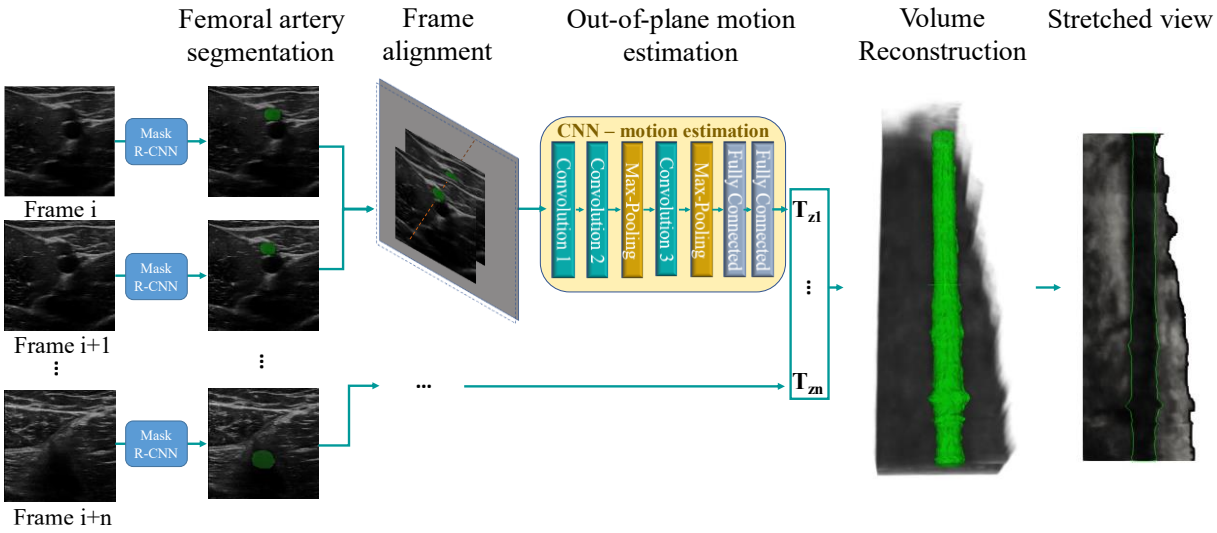


Fig. 1. Overview of the global workflow.

Accepted manuscript / Final version

2.3 Out Of Plane Motion Estimation

Because neural networks need a fixed input size, an input placeholder of 2 channels was created with enlarged height and width so it could contain an aligned pair of frames. The first frame was centered in the placeholder's first channel. Then, the second frame was included by aligning both barycenters. The contrast of all input frames was improved using contrast limited adaptive histogram equalization (CLAHE).

The network predicts the relative longitudinal motion (in mm) between the input registered pair of frames. The CNN contains 3 convolutional layers, 2 max-pooling layers, and 2 fully connected layers. Regarding the limited size of our database and the single out-of-plane translation to estimate, 3 convolutional layers were sufficient to prevent overfitting and reduce the complexity of the extracted features. The L1 loss function was used as the criterion to be minimized during training.

5-fold cross-validation was used for training and validation. This validation process has been shown to be statically relevant for such small datasets [17]. For each fold, the whole 111 tracked US sequences of the 18 volunteers were used and split into 10 volunteers for training, 4 volunteers for validation, and 4 volunteers for testing. Each set contained data acquired by both operators. Between 13087 and 15687, 4323 and 4916, and 4058 and 5789 consecutives pairs of original frames were obtained for each fold for training, validation, and testing respectively. Data augmentation was eventually applied by horizontally mirroring each frame during the training phase. The network was implemented by using the publicly available Pytorch library. The Adam optimizer was with a fixed learning rate of 1×10^{-4}. The input placeholder shape was set to 530×530 to allow all our training pairs to be aligned. All the models converged between 13 and 16 epochs.

2.4 Stretched Reconstruction

All frames were aligned according to the position of the femoral artery, by centering the segmentation mask on all frames. The out-of-plane motion, provided by the CNN, allowed building a 3D volume, with the femoral artery at its center. Since the images are not uniformly spaced in the out-of-plane axis, a linear interpolation is applied to generate the final volume. Finally, 2d cutting planes centered on the femoral artery were generated to produce visualizations of the full artery lumen.

Two metrics were used for evaluating 3D reconstructions. The relative frame-to-frame longitudinal error, which represents the absolute difference between the estimation of our CNN and the ground truth acquired through the optical tracker, was employed. In addition, the final drift error was also used to evaluate the impact of error accumulation. The final drift error refers to the absolute difference between the position of the last frame of the volume reconstructed with the position provided by the tracker (i.e., ground truth) compared to the position calculated with the network outputs.

Only sequences longer than 10 cm were considered to compute the drifts errors, representing 70% of all our sequences. Our method was compared to a naïve method and a 1-axis CNN. The naïve method, also called the linear motion method, consisted of computing the average out-of-plane translation on the training dataset and applying it to each frame of a sequence. The 1-axis CNN corresponds to the same network used in our method but without artery alignment, by simply taking each pair of consecutives frames as input.

Accepted manuscript / Final version

3 Experiments and Results

3.1 Femoral Artery Segmentation

The network was trained during 30 epochs. On the testing database of 1004 frames, our network reached a false negative rate of 7% and a mean dice score of 0.90 computed on the true positive cases. Only two frames presented a false positive detection, where the network segmented the genicular artery bifurcation instead of the femoral artery. Example of artery segmentation results are shown in Fig. 2. The inference time was relatively low with an average of 0.85s per frame on a standard CPU.

3.2 Out-of-plane Movement Estimation and Stretched Reconstruction Evaluation

Results of the stretched reconstruction method in comparison with other methods are summarized in Table 1. The proposed method presents similar precision in term of average absolute error than the CNN without artery alignment. However, it results in a statistically significant lower final drift with an average drift of 17.45mm. Because the total lengths of the sequences can vary (between 102 and 272 mm), final drift errors, expressed as percentages of the total artery's length, are depicted in Fig. 3. Paired two-sample *t*-tests were performed, and *p*-values of less than 0.01 between our method and the other method were obtained. Examples of final stretched views reconstructed with the different methods and the absolute position error of frames in the sequences are illustrated in Fig. 4.

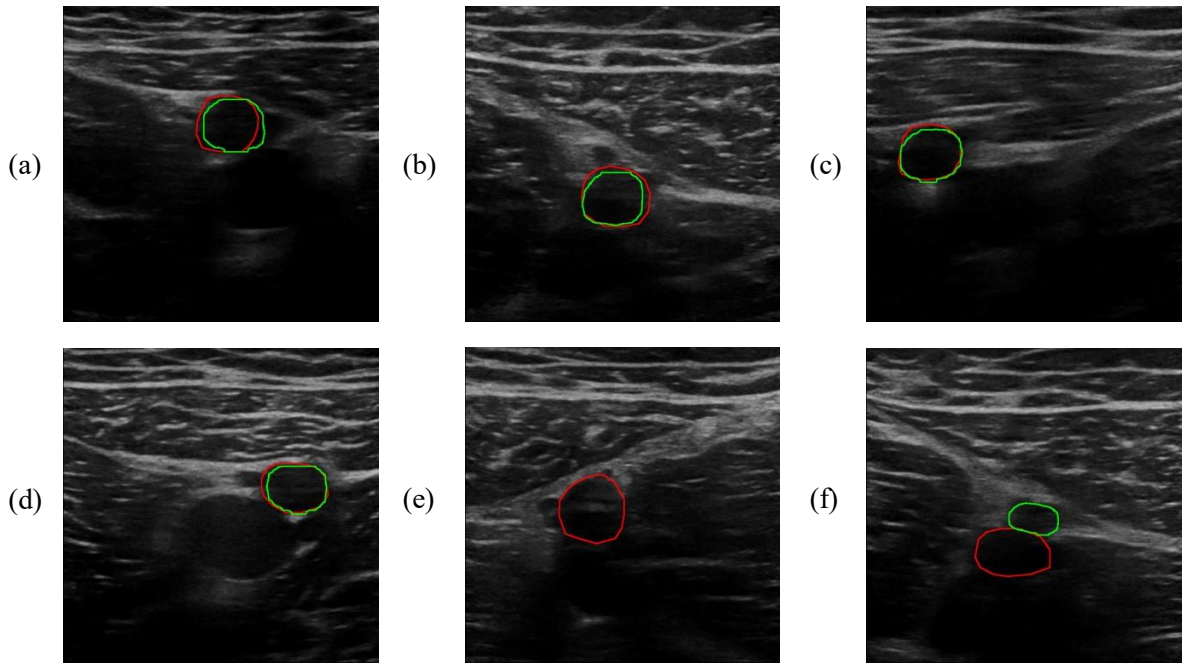


Fig. 2. Examples of the mask R-CNN segmentation results on test frames with the ground truth delimited in red and the inference segmentation in green. (a, b, c, d) True positives detections (93% of the database) with dice scores of 0.85, 0.88, 0.92 and 0.92 respectively. (e) False negative case (7%). (f) A case of both false negative and false positive (0.2%) case where the network segments the genicular bifurcation of the femoral artery.

Accepted manuscript / Final version

Table 1. Performance results of different methods on the femoral artery dataset (test set).

Methods	Frame to frame out-of-plane translation error (mm)				Final drift error (mm)			
	Min	Median	Max	Average	Min	Median	Max	Average
Linear Motion	0	0.32	4.06	0.40	2.6	33.18	105.26	37.43
1-axis CNN	0	**0.19**	3.19	**0.27**	**0.05**	17.12	82.90	19.75
1-axis CNN with artery alignment	0	0.2	**2.85**	0.28	0.18	**13.42**	**68.31**	**17.22**

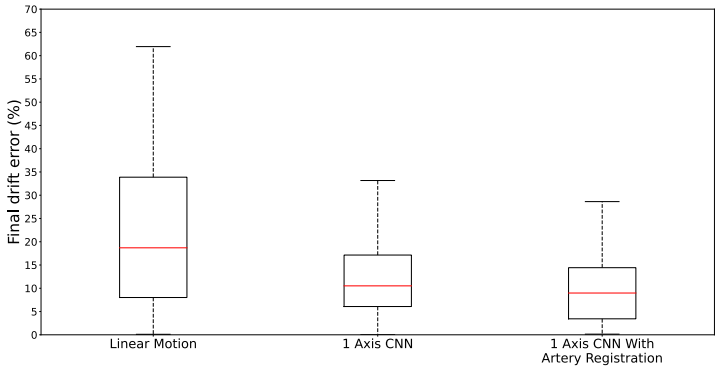


Fig. 3. Comparison of reconstruction methods according to final error drift rates per sequence.

The average inference time for a pair is 1ms. Taking into account the segmentation process, around 0.85s is needed to process a new frame with our method.

4 Discussion

A complete method for generating stretched reconstruction of the femoral artery is presented. The generated volumes provide rich diagnosis information. Planes can easily be extracted to give a direct visualization of the artery allowing fast artery diameter measurement and lesion sizing.

The proposed approach was compared to a naïve method of applying a single inter-frame distance calculated on the training database. It would have been of interest to adapt this method by measuring the total length of each sequence at the time of acquisition and using this length to estimate an interframe distance for each sequence. While this method would reduce the final drift error, it would suffer from potential inaccuracies when measuring the total length and would remain limited in case of sequences with speed variations.

Our method was not compared to 6 degrees of freedom CNN [9] since it disregards orientation and approximates in-plane motion by centering the artery. Thus, the reconstructed volume contains anatomical deformations beside the artery, whereas the 6 degrees of freedom CNN is designed to build a full US volume. The impact of not considering orientation in our reconstruction method was estimated by extracting orientation through all sequence acquisitions with the optical tracker. The three Euler angles have been computed and the absolute difference between 2 successive frames in all the sequences in our database was on average 0.07, 0.07, 0.08 degrees for roll,

Accepted manuscript / Final version

pitch, and yaw, respectively. The relatively small rotational motion in our sequences demonstrates the low tortuosity of the femoral artery and justifies ignoring orientations in our method.

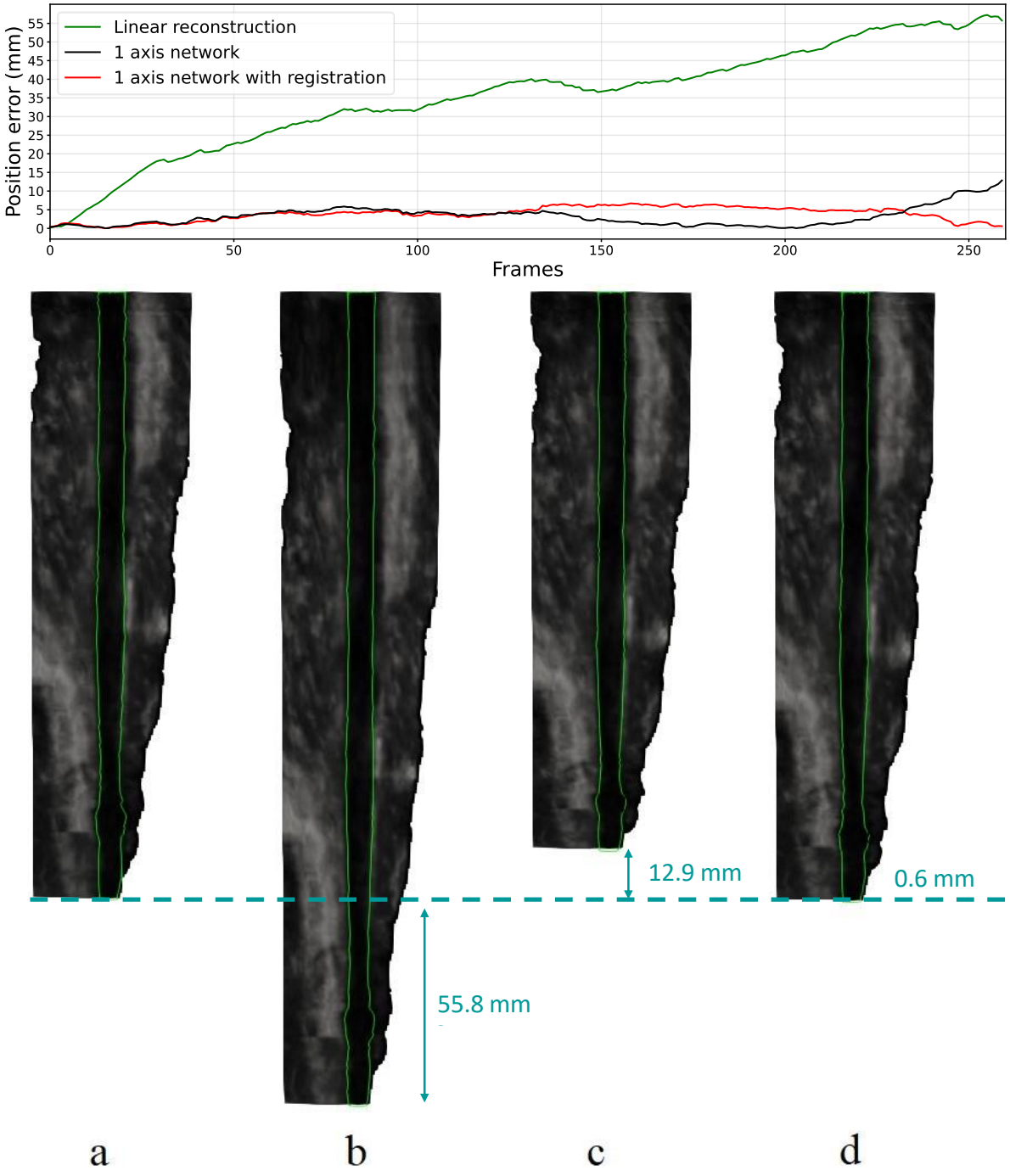


Fig. 4. A good case of final stretched views of the femoral artery where the out-of-plane motion was provided by ground truth (a), linear motion (b), 1-axis CNN (c), 1-axis CNN with artery registration (d) and the corresponding drifts errors. The absolute frame position errors of the reconstructed views are represented in the graph. The final drift error of the 1 axis CNN with artery segmentation is 0.6 mm. The artery is delimited in green. All stretched views were built from artery-centered frames to allow artery visibility.

Accepted manuscript / Final version

The results on femoral artery segmentation are satisfying considering the small size of our training database (2073 frames). To minimize false negatives, some ground truth segmentations were made on frames where the femoral artery was not distinctly visible. The segmentation gives a clear view of the artery and allows direct quantitative measurements of diameters.

Many hyperparameters had to be optimized to design the out-of-plane motion CNN. Tests were performed on the number of convolution layers, the size of fully connected layers, or the type of optimizer to use. Experiments were also carried out by including pairs of non-consecutives frames, but it degraded the performance of the network. The network was also evaluated using the L2 loss to minimize frame to frame large errors but without success. Extra channels have been added to the input to add the optical flow field using Farnebäck estimation, but it didn't improve the network performance since it only focuses on out-of-plane translation. The consistency loss function was not tested for the same reason. 80% of the test database showed a final drift of less than 15% with our reconstruction method, which is compatible with lesion lengths computation in PAD procedures. The high maximum final drift errors came from sequences for which the operator scanned the artery with more abrupt gestures. The final drift error is particularly meaningful for our application since it measures the length error of the reconstructed artery and evaluates the cumulated error. Experiments were performed on input frame pixel size concluding that a resolution of 0.15 mm was optimal. Higher resolution led to too large input frames and limited our batch size. Lower pixel size degraded input image information and decreased our final precision. The two CNN-based reconstruction methods outperformed the linear motion approach. The artery alignment before the estimation of the out-of-plane motion had a positive influence on the result. A significant in-plane motion was observed: for each centimeter of longitudinal displacement, an averaged in-plane displacement of 1.14, and 2.13 mm for the left-right and the anteroposterior axis, respectively, were measured. Even if the segmentation process is time-consuming, the time needed to generate stretched views for a sequence is still compatible with pre-operative constraints.

The US frames used in this work were grabbed after the echograph processing when the frames are displayed on the operator screen. Speckle filtering was strongly reduced, but speckle reduction was still present. Assessing original data before the echograph processing could certainly be of interest to capture other features in frames and improve the network performance.

Tests still have to be performed on the use of a 3D CNN with 3D kernels to use more than 2 consecutives frames as input to estimate the global transformation as in [12]. A sensibility study on patients suffering from PAD is also needed to evaluate the diagnostic capabilities of this approach. If the added value of this approach for pre-operative planning of PAD procedures is clear, the integration in the intra-operative workflow would need further works. The registration of intra-operative live 2D US frame on the pre-operative stretched reconstruction could guide the surgeon during the procedure, leading to contrast-free and radiation-free PAD procedures.

The artery is distinctly visible on stretched views showing its diagnosis interest. Fig. 5 shows an example of diameter measurement through a sequence using the segmentation masks. The sequence was acquired by a third operator on a patient with benign hypoechoic plaques. A non-pathological narrowing of the artery can be seen at 175 mm. Stretched views allow to directly identify, locate, and size lesions in terms of diameter and length. This work is the first step to integrate 3D US reconstruction in the PAD procedure workflow and patient care. The stretched view can be useful in the pre-operative diagnosis and procedure planning to identify and map all lesions in a more efficient and visual manner than the actual clinical workflow, which often only includes 2D frames. These representations could be directly integrated into the patient record. It could be a strong alternative to MRA

Accepted manuscript / Final version

or CTA in terms of cost and ease of use, but also to the intra-operative arteriography. The proposed method could encourage to routinely perform pre-operative sizing in PAD procedures.

5 Conclusion

This paper introduced a deep-learning-based stretched reconstruction method from 2D freehand US for PAD. An initial in-plane alignment based on the segmentation of the femoral artery before estimating the out-of-plane translation is proposed. Our method showed superior performance compared to other methods in terms of drift error. The generated views can be integrated into the patient record and offer a clear visualization of the patient's anatomy to the surgeon.

Conflict of Interest: The authors declare that they have no conflict of interest.

Ethical approval: For this type of study formal consent is not required.

Informed consent: Informed consent was obtained from all individual participants included in the study.

Accepted manuscript / Final version

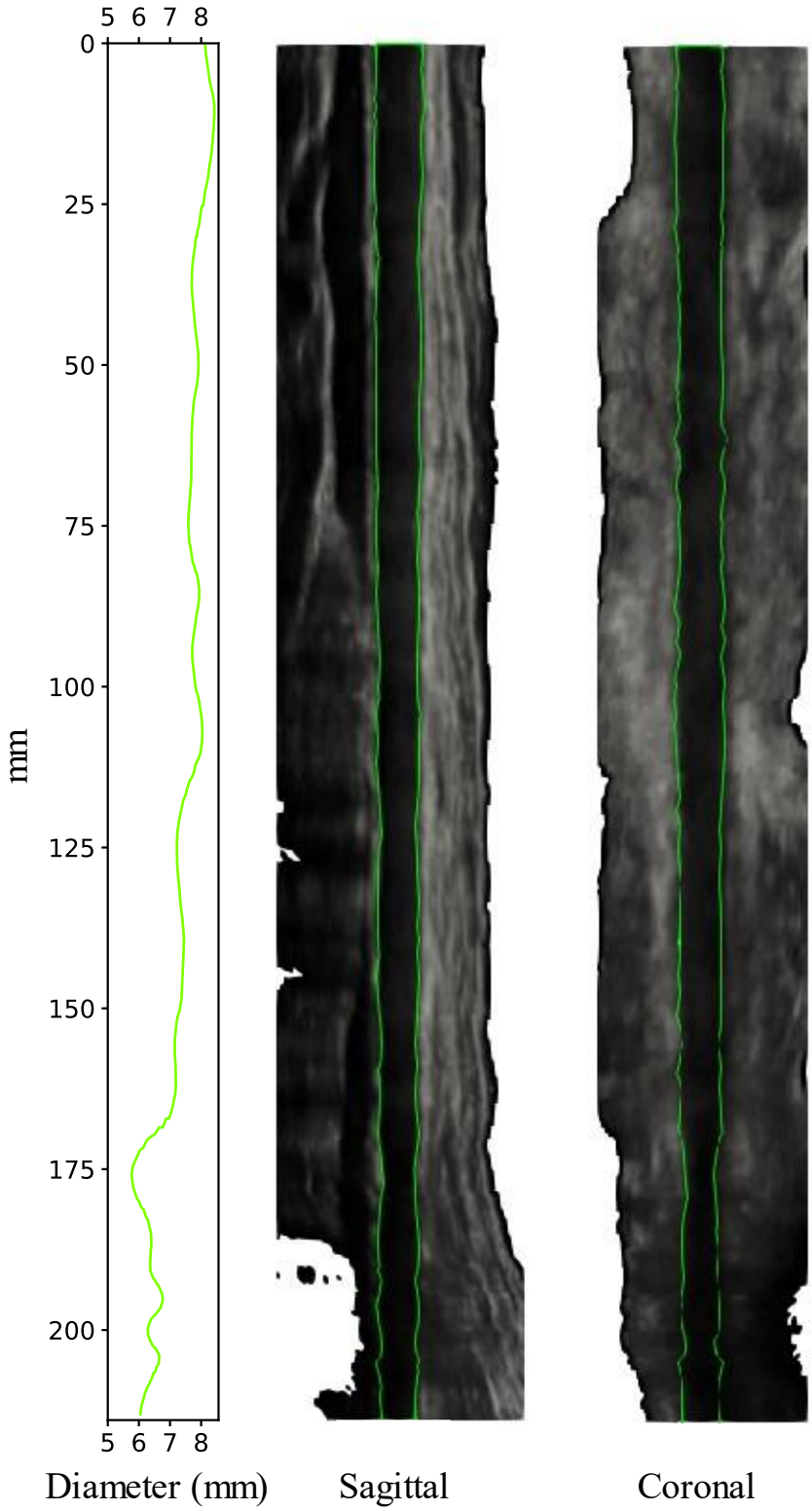


Fig. 5. Example of the femoral artery's diameter measurement through a sequence. Stretched views of the corresponding sequence are represented on the right in the sagittal and the coronal plane.

Accepted manuscript / Final version

References

1. Norgren, L., Hiatt, W.R., Dormandy, J.A., Nehler, M.R., Harris, K.A., Fowkes, F.G.R., TASC II Working Group: Inter-Society Consensus for the Management of Peripheral Arterial Disease (TASC II). J. Vasc. Surg. 45 Suppl S, S5-67 (2007). https://doi.org/10.1016/j.jvs.2006.12.037.

2. TASC Steering Committee, Jaff, M.R., White, C.J., Hiatt, W.R., Fowkes, G.R., Dormandy, J., Razavi, M., Reekers, J., Norgren, L.: An Update on Methods for Revascularization and Expansion of the TASC Lesion Classification to Include Below-the-Knee Arteries: A Supplement to the Inter-Society Consensus for the Management of Peripheral Arterial Disease (TASC II). Vasc. Med. Lond. Engl. 20, 465–478 (2015). https://doi.org/10.1177/1358863X15597877.

3. Conte, M.S., Bradbury, A.W., Kolh, P., White, J.V., Dick, F., Fitridge, R., Mills, J.L., Ricco, J.-B., Suresh, K.R., Murad, M.H., GVG Writing Group: Global vascular guidelines on the management of chronic limb-threatening ischemia. J. Vasc. Surg. 69, 3S-125S.e40 (2019). https://doi.org/10.1016/j.jvs.2019.02.016.

4. Mohamed, F., Vei Siang, C.: A Survey on 3D Ultrasound Reconstruction Techniques. Presented at the April 27 (2019). https://doi.org/10.5772/intechopen.81628.

5. Neshat, H., Cool, D.W., Barker, K., Gardi, L., Kakani, N., Fenster, A.: A 3D ultrasound scanning system for image guided liver interventions. Med. Phys. 40, 112903 (2013). https://doi.org/10.1118/1.4824326.

6. Chung, S.-W., Shih, C.-C., Huang, C.-C.: Freehand three-dimensional ultrasound imaging of carotid artery using motion tracking technology. Ultrasonics. 74, 11–20 (2017). https://doi.org/10.1016/j.ultras.2016.09.020.

7. Zielinski, A.H., Bredahl, K.K., Ghulam, Q., Rouet, L., Dufour, C., Sillesen, H.H., Eiberg, J.P.: Full-Volume Assessment of Abdominal Aortic Aneurysms by 3-D Ultrasound and Magnetic Tracking. Ultrasound Med. Biol. 46, 3440–3447 (2020). https://doi.org/10.1016/j.ultrasmedbio.2020.09.002.

8. Prevost, R., Salehi, M., Sprung, J., Ladikos, A., Bauer, R., Wein, W.: Deep Learning for Sensorless 3D Freehand Ultrasound Imaging. In: Descoteaux, M., Maier-Hein, L., Franz, A., Jannin, P., Collins, D.L., and Duchesne, S. (eds.) Medical Image Computing and Computer-Assisted Intervention − MICCAI 2017. pp. 628–636. Springer International Publishing (2017).

9. Prevost, R., Salehi, M., Jagoda, S., Kumar, N., Sprung, J., Ladikos, A., Bauer, R., Zettinig, O., Wein, W.: 3D freehand ultrasound without external tracking using deep learning. Med. Image Anal. 48, 187–202 (2018). https://doi.org/10.1016/j.media.2018.06.003.

10. Dupuy, T., Beitone, C., Troccaz, J., Voros, S.: 2D/3D Deep Registration for Real-Time Prostate Biopsy Navigation. In: SPIE Medical Imaging 2021. SPIE, Digital congress, United States (2021). https://doi.org/10.1117/12.2579874.

11. Miura, K., Ito, K., Aoki, T., Ohmiya, J., Kondo, S.: Localizing 2D Ultrasound Probe from Ultrasound Image Sequences Using Deep Learning for Volume Reconstruction. Presented at the October 1 (2020). https://doi.org/10.1007/978-3-030-60334-2_10.

12. Guo, H., Xu, S., Wood, B., Yan, P.: Sensorless Freehand 3D Ultrasound Reconstruction via Deep Contextual Learning. ArXiv200607694 Cs Eess. (2020).

Accepted manuscript / Final version

13. Luo, M., Yang, X., Huang, X., Huang, Y., Zou, Y., Hu, X., Ravikumar, N., Frangi, A.F., Ni, D.: Self Context and Shape Prior for Sensorless Freehand 3D Ultrasound Reconstruction. ArXiv210800274 Cs Eess. (2021).

14. Kaladji, A., Giovannetti, M., Pascot, R., Clochard, E., Daoudal, A., Lucas, A., Cardon, A.: Preoperative CT-scan-based sizing and in-stent restenosis in peripheral endovascular revascularizations. Vascular. 25, 504–513 (2017). https://doi.org/10.1177/1708538117700764.

15. Lasso, A., Heffter, T., Rankin, A., Pinter, C., Ungi, T., Fichtinger, G.: PLUS: Open-Source Toolkit for Ultrasound-Guided Intervention Systems. IEEE Trans. Biomed. Eng. 61, 2527–2537 (2014). https://doi.org/10.1109/TBME.2014.2322864.

16. Torralba, A., Russell, B.C., Yuen, J.: LabelMe: Online Image Annotation and Applications. Proc. IEEE. 98, 1467–1484 (2010). https://doi.org/10.1109/JPROC.2010.2050290.

17. Pasini, A.: Artificial neural networks for small dataset analysis. J. Thorac. Dis. 7, 953–960 (2015). https://doi.org/10.3978/j.issn.2072-1439.2015.04.61.

Accepted manuscript / Final version